UNCLASSIFIED

(2)

AD-A212 183

DTIC ELECTE SEP 11 1989 B

DOCUMENTATION PAGE

Form Approved OMB No. 0704-0188

1b. RESTRICTIVE MARKINGS

3. DISTRIBUTION/AVAILABILITY OF REPORT
APPROVED FOR PUBLIC RELEASE
DISTRIBUTION IS UNLIMITED

2b. DECLASSIFICATION/DOWNGRADING SCHEDULE

4. PERFORMING ORGANIZATION REPORT NUMBER(S)

5. MONITORING ORGANIZATION REPORT NUMBER(S)
AFOSR-TR- 89-1228

6a. NAME OF PERFORMING ORGANIZATION
Tel-Aviv University

6b. OFFICE SYMBOL (If applicable)

7a. NAME OF MONITORING ORGANIZATION
AFOSR/NA

6c. ADDRESS (City, State, and ZIP Code)
Ramat-Aviv
Tel-Aviv, 69978, Israel

7b. ADDRESS (City, State, and ZIP Code)
BUILDING 410
BOLLING AFB, DC 20332-6448

8a. NAME OF FUNDING/SPONSORING ORGANIZATION
AFOSR/NA

8b. OFFICE SYMBOL (If applicable)
NA

9. PROCUREMENT INSTRUMENT IDENTIFICATION NUMBER
AFOSR-86-0323

8c. ADDRESS (City, State, and ZIP Code)
BUILDING 410
BOLLING AFB, DC 20332-6448

10. SOURCE OF FUNDING NUMBERS

PROGRAM ELEMENT NO.	PROJECT NO.	TASK NO	WORK UNIT ACCESSION NO.
61102F	2307	A2	

11. TITLE (Include Security Classification)
(U) The Delay of Turbulent Boundary Layer Separation by Oscillatory Active Control

12. PERSONAL AUTHOR(S)
Y. Katz, B. Nishri, I. Wygnanski

13a. TYPE OF REPORT	13b. TIME COVERED	14. DATE OF REPORT (Year, Month, Day)	15. PAGE COUNT
FINAL	FROM AUG 87 TO OCT 88	4 April 89	17

16. SUPPLEMENTARY NOTATION

17. COSATI CODES			18. SUBJECT TERMS (Continue on reverse if necessary and identify by block number)
FIELD	GROUP	SUB-GROUP	Separation, Turbulence, Boundary Layers, Stall

19. ABSTRACT (Continue on reverse if necessary and identify by block number)

The flow over a solid wedge from which a fully developed turbulent boundary layer separates naturally, was investigated experimentally. The flow which separates at the geometric discontinuity turns into a free mixing layer downstream of it. However the flow can be forced to reattach by the introduction of two-dimensional, harmonic, and small-amplitude perturbations at the apex of the wedge. The temporally-averaged characteristics of the reattached boundary layer are typical to flows at less severe pressure gradients, with the exception of the spanwise cohenence near the solid surface which has been notably enmhanced by the imposed perturbations. Phase-locked and ensemble-averaged results indicate that the subharmonic frequency dominates the flow at large distances from the apex.

20. DISTRIBUTION/AVAILABILITY OF ABSTRACT
☐ UNCLASSIFIED/UNLIMITED ☒ SAME AS RPT. ☐ DTIC USERS

21. ABSTRACT SECURITY CLASSIFICATION
UNCLASSIFIED

22a. NAME OF RESPONSIBLE INDIVIDUAL
JAMES M MCMICHAEL

22b. TELEPHONE (Include Area Code)
202-767-4935

22c. OFFICE SYMBOL
AFOSR/NA

DD Form 1473, JUN 86 Previous editions are obsolete. SECURITY CLASSIFICATION OF THIS PAGE

UNCLASSIFIED

THE DELAY OF TURBULENT BOUNDARY LAYER SEPARATION BY OSCILLATORY ACTIVE CONTROL

by

Y. Katz, B. Nishri, and I. Wygnanski

ABSTRACT

The flow over a solid wedge from which a fully developed, turbulent boundary layer separates naturally, was investigated experimentally. The flow which separates at the geometric discontinuity turns into a free mixing layer downstream of it. However the flow can be forced to reattach by the introduction of two-dimensional, harmonic, and small-amplitude perturbations at the apex of the wedge. The temporally-averaged characteristics of the reattached boundary layer are typical to flows at less severe pressure gradients, with the exception of the spanwise coherence near the solid surface which has been notably enhanced by the imposed perturbations. Phase-locked and ensemble-averaged results indicate that the subharmonic frequency dominates the flow at large distances from the apex at all forcing frequencies considered thus far.

The preliminary results presented, indicate that this might be an effective way to delay separation of turbulent as well as laminar boundary layers.

INTRODUCTION

The maximum lift generated by airfoils and the maximum divergence angles of efficient diffusers are limited by flow separation. Consequently, even a partial control of separation represents a formidable challenge to the aeronautical and mechanical engineer. The upper surface of many high-lift airfoils is specially contoured in order to maintain attached flow at high angles of attack.

Some airfoils are designed to stall gently[1-3] by initiating the separation near the trailing edge and allowing it to creep upstream with increasing angle of attack, while other designs traded off this beneficial feature in favor of a higher lift coefficient or a lower pitching moment coefficient. Nevertheless the maximum lift coefficient generated by a single-element airfoil seldom exceeds the value of 1.8 at the designed range of Reynolds numbers. The performance of most airfoils degrades rapidly at low Reynolds numbers where various tripping devices are commonly used in order to promote transition to turbulence before the occurance of separation. Stationary elements like flaps and slats which alter the geometry of the airfoil are therefore used at low forward speeds despite of their bulk and the comlexity of their mechanical actuators. Active devices which alter the mean flow in the boundary layer by adding or removing fluid through suction or blowing never caught-on because of their cumbersome size and unreliable nature. The introduction of small-amplitude, *oscillatory motion* for control of separation may be attractive whenever the mean flow is unstable to the imposed oscillations and amplifies them. The apparatus necessary in this case, might be small and simple and therefore attractive to industry.

Preliminary observations made on two-dimensional airfoils[1,2] indicate that small vibrating ribbons flaps or fences, whose overall dimensions are less than 2% of the airfoil chord, oscillating at a reduced frequency of approximatly 2 [i.e. at $F^+ = fc/U = 2$ where c is the airfoil chord and U is the free stream velocity] delayed the incidence at which stall occurred and increased the maximum lift generated by these airfoils. For example, the streakline pattern shown in figure 1a indicates that the flow on a NACA 0015 airfoil inclined to the free stream at an angle of attack of 16 o is completely separated. The flow reattached to the surface when a small flap, located near the leading edge of the airfoil (figure 1b), was forced to oscillate at a displacement amplitude which was smaller than 1% of the chord. The application of active control has its roots in the work of Oster et al.[3], where a similar method applied to a mixing layer showed a marked increase in the spreading rate of that flow and thus an increase in the rate of entrainment of fluid into the turbulent zone. Whenever the entrained fluid comes from a limited reservoir bound by the mixing layer on one side and

by the solid surface on the other, the pressure in that reservoir drops and the pressure gradient which is generated across the flow bends the mixing layer towards the surface. Consequently, enhancing the rate of entrainment may delay separation or promote reattachment.

In another experiment, a high performence airfoil[4] shown in figure 2a experienced a terrible lift hysteresis whenever the $Re<4 10^5$ and the angle of attack exceeded 30^0 (figure 2b). The angle of attack at which the airfoil recovered from stall under these conditions was 7^0 and the minimum C_L prior to recovery is 0.48. Taking this airfoil beyond the stall angle implies a substantial loss of lift equivalent to $\frac{3}{4}$ of the maximum lift coefficient generated by this airfoil prior to stall. A transition strip reduced the extend of the hysteresis loop but also degraded the performance of the airfoil by reducing the maximum C_L generated. A stationary "flaperon" protruding 1 mm. above the surface and may be regarded as a large two-dimensional transition strip reduced the maximum lift coefficient to 1.05 without eliminating the hysteresis entirely at $Re=3 10^5$. Oscillating the flaperon at a reduced frequency $F^+ = 1.6$ recovered most of the lift (i.e. $C_{Lmax.} = 1.6$) and eliminated the hysteresis loop entirely (figure 2b). At lower Reynolds numbers [e.g.$Re=10^5$], the maximum lift coefficient of the basic airfoil degenerated to approximately 0.5 and typical transition strips did not menage to enhance it byond 0.7 (fig 3) while a vibrating fence emerging from the interior of the airfoil recovered the lift which is otherwise generated at much higher Re. All this was acomplished with a concomitant reduction of the drag coefficient (see also figures 21-26 in reference 4).

Since the detailed character of the boundary layer depends on the geometry of the airfoil and on the Reynolds number, it is rarely of universal interest, while the *principle of active control of the boundary layer separation* by oscillatory means is in that category. One may contend that reattachment may occur provided the separated boundary layer is laminar and it undergoes transition downstream of separation. If this was the only condition for reattachment, then vortex-generators and other tripping devices used in reference 4 could have been equally effective in delaying separation, while no control would have been feasible whenever the upstream flow is turbulent. The present study was undertaken in order to test the feasibility of actively delaying the separation of a turbu-

lent boundary layer.

EXPERIMENTS

The mixing layer facility[3] was modified to suit this investigation. A flat plate 75 cm long was hinged to the splitter plate (figure 4) and provided a discontinuity in the surface which initiated separation under normal circumstances. The extent of the separated region depends on the length of the protruding surface to which a small flaperon was attached and on the relative angle of the stationary flaperon with the surface. Although the inclination angle of the plate was adjustable, the results described presently correspond to an inclination of 18 and a protrusion of 10mm to which 10mm flaperon was attached. The stationary flaperon was aligned with the splitter plate and formed a smooth extension of it's surface. Boundary layer coordinates for which X is parallel to the inclined plate and Y is normal to it were used, and the traversing mechanism which is normally driven in a coordinate system established by the splitter plate was programed to account for this inclination angle. The surface of the splitter plate was roughened some 100 boundary layer thicknesses upstream in order to ensure transition and to thicken the upstream boundary layer. The flaperon was made of a thin sheet metal and spanned the entire test section. In the absence of the forced oscillations, the flow separated at the trailing edge of the flap and failed to reattach to the inclined flat-plate at the inclination angles considered. The severity of the separation [or the height of the separated region] was sensitive to the stationary angle of the flap whose trailing edge determined the vertical distance of the inital mixing-layer above the inclined surface. The displacement amplitudes of the flap were of the order of ± 1 mm. The imposed streamwise component of velocity oscillations were measured by a hot-wire located in the potential flow near the flap (figure 4). The velocity perturbation was recorded together with the forcing signal, and the data were ensemble-averaged in order to remove the free stream turbulence of the wind tunnel and other sources of random disturbances from contaminating the results.

The boundary layer approaching the discontinuity was carefully mapped at four stations across the span. The mean flow is two-dimensional (figure 5) and the velocity profiles are typical for a turbulent boundary layer in this range of Reynolds numbers (i.e., the shape factor $H \equiv \delta^*/\theta = 1.6$ for $Re_{\delta^*} = 800$). The maximum turbulent intensity, u'/U is approximately 7% 50 mm upstream of the hinge and it increases to 15% 10 mm upstream.

The flow generated downstream of separation resembles the classical, unforced mixing layer[5] observed in the absence of pressure gradient. The locus of points at which the velocity is equal to 1/2 of the local free stream velocity outside boundary layer and which traditionally defines the center of the flow is inclined to the splitter plate at an angle of 15 o. Since this angle does not change appreciably with X, the "dead water region" has a shape of a wedge. The vorticity thickness, δ_v, obtained by fitting a straight line to the mean velocity profile at the point of inflexion[5] increases linearly with X, as it does in the classical mixing layer. The slope of the vorticity thickness $d\delta_v/dX = 0.23$ is in good agreement with previously made measurements in which the boundary layer on the splitter plate was tripped.[6]

The conventional use of hot-wires for measuring velocity is not meaningful in the recirculating region and its vicinity, i.e., for $\overline{Y} \equiv (Y - Y_{0.5})/\delta_v < 0.5$. However, since we did not intend to study the reecirculating flow in this investigation, the "constant velocity" perceived as a result of the rotation of the flow was simply referred to as U_{min}. It is approximately equal to 17% of the free stream velocity U_{max} and it occurs between $-1.5 < \overline{Y} < -0.7$. The dimensionless distribution of $(U - U_{min})/(U_{max} - Umin)$ vs. $\overline{Y}$ is plotted in figure 6 and compared with the corresponding analytic expression representing the mean velocity profile used in the mixing layer between two parallel streams.[7] The quality of this representation suggests that the separated flow is no different from the classical mixing layer and thus it can be externally excited in the same manner as was the plane mixing layer. The pressure recovery coefficient $C_p \equiv (P - P_{init})/1/2\rho U^2_{init}$ was approximately 0.1 over the distance of 60 cm and provided an additional indication that the flow was fully separated (figure 7).

Activating the flap at frequencies corresponding to Strouhal numbers based on initial momentum thickness [$St \equiv f\theta/U]_{init}$, which are smaller than 0.01 and reference amplitudes $u'/U_{init} < 0.25\%$, resulted in a complete reattachment of the flow to the surface and a pressure recovery expressed by $C_p \simeq 0.5$ over the corresponding distance considered before (figure 7). The flow was partially reattached at reference amplitudes as low as 0.1%, as may be deduced from the respective values of the C_p measured along the surface (figure 7). One may conclude, therefore, that the externally introduced oscillations were sufficiently amplified to allow the boundary layer to overcome the adverse pressure gradient imposed by the divergence of the walls.

The dependence of some important boundary layer parameters, like the momentum thickness θ, the shape factor H, and the skin-friction coefficient C_f, on X is plotted in figure 8 for the 3 frequencies tested to date and for the 3 amplitudes at f = 40 hz. It is hardly surprising that the momentum thickness increases monotonically with X and it does so more rapidly than on a corresponding flow over a flat plate in the absence of pressure gradient. The shape factor decreases initially with X and then gradually increases towards the trailing edge of the plate, while the skin friction coefficient behaves in an opposite fashion. The X location at which H is smallest corresponds to the location at which C_f is largest, as might have been expected from the momentum integral equation provided the pressure increases monotonically with X. The location at which H has a minimum appears to depend primarily on the frequency of forcing and not on the amplitude, while the minimum value of H attained depends mostly on the amplitude of the imposed oscillations. The value of fX/U at which H attains its minimum is approximately 2, suggesting that the wave-length of the imposed oscillations determines the preferred reattachment distance. Since the maximum lift on the airfoils tested [i.e. the NACA 0015; the Wortmann FX63-137 and the IAI P255] was also generated at approximately the same Strouhal number, in spite of the fact that the separating boundary layer in the latter cases was an order of magnitude thinner and more often than not laminar, suggests that the mechanism affecting reattachment must be quite independent of the detailed structure of the boundary layer upstream of separation. When the frequency is reduced (f = 20 hz) so that the

Strouhal number of 2 is attained near or byond the trailing edge of the inclined plate, another length parameter [corresponding to the finite length of the plate] is introduced whose effects are not as yet clearly understood. It is clear, however, that the neither H nor C_f recovers to its initial value measured upstream of the hinge in spite of the fact that the highest pressure coefficient is recovered at this frequency. The frictional losses, in this case, are almost 100% smaller than for the same initial amplitudes of forcing at f = 40 or 80 hz and are comparable to forcing amplitudes of 0.25% at the frequency of 40hz (figure 8c). Consequently, the boundary layer forced at f = 20hz might be closer to separation than it is at the other frequencies considered, although it is still far removed from the intermittent separation correlation of Sandborn and Kline[8] since H < 2.

Representative mean velocity and turbulent intensity profiles measured at X = 35 cm are plotted in figure 9 for the 3 frequencies considered at a forcing amplitude of 1%. These profiles are typical of boundary layers evolving at moderately adverse pressure gradients[9] with the exception of the maximum level of turbulence which attains almost 20% and is more characteristic of the level measured in separated flows.[10] When the mean velocity profiles are plotted in the usual "law-of-the-wall" coordinates the universal logarithmic distribution remains unchanged regardless of the forcing frequency or amplitude. The maximum value of Y^+ which the equation may be fitted depends not only on the pressure gradient but also on the amplitude and the frequency of forcing and can be best correlated with the dependence of H on these parameters:

$$U^+ = 5.6 \log Y^+ + 5 . \tag{1}$$

The general representation of the "law-of-the-wake" also applies in all cases considered, i.e.,

$$W = C \sin^2\left[\Pi \frac{Y}{2\delta}\right], \tag{2}$$

but the constant C depends on the frequency and the amplitude of the forcing and correlates well

with the value of H attained. For example:

X	f	A	H	$[Y^+]max$	C
30 cm	40 hz	1%	1.5	250	6.7
20 cm	80 hz	1%	1.57	150	9.4
30 cm	40 hz	0.25%	1.77	100	23.0

These results might be deduced from the data shown in figure 10.

When the amplitude of the oscilations was so small that the boundary layer was incapable of negotiating the pressure gradient without separating (i.e., at f = 40 hz and A = 0.1%; see figure 7), the wake component could not be fitted with the universal function given in equation 2, while the "law-of-the-wall" still applied (figure 11). The wake component of the boundary layer is, therefore, mostly affected by the imposed oscillations.

The ensemble-averaged velocities plotted in figure 12a-c are phase-locked to the imposed oscillations shown at the bottom left corner of each figure. These ensembled time series indicate that a large fraction of the fluctuations are correlated to the motion of the flap and are coherent across the boundary layer. They represent velocities measured at various Y locations during two periods of the forcing frequency. The amplitudes and the relative phases of the fundamental (forced) frequency are plotted to the right of these series in figure 12. These distributions suggest that the fundamental frequency may be viewed as an array of spanwise vortices extending across the entire boundary layer. The 180 shift in phase which depicts the center of the eddy is convected along the surface at approximately one-half of the free stream velocity and it is convected away from the surface with increasing X. The amplitude distribution observed across the boundary layer appears to conform with the expected eigenfunctions based on the linear stability analysis. Fourier analysis of the phase-locked signals (figure 13) reveals that the maximum value of the fundamental frequency at a given X station decreases rapidly with increasing distance downstream of the flap, as does also the

first harmonic of the velocity perturbation. The decrease in this maximum should not be construed as a decrease in the overall level of energy contained in this frequency but rather as a redistribution of energy resulting from a change in the shape of the eigenfunction stemming from the rapid divergence of the flow. The integrated subharmonic content of the signal remains approximately constant and even amplifies somewhat with increasing X. The subharmonic always dominates the flow at distances which are larger than the X location at which the shape factor H attains its minimum The emergence of the subharmonic as the dominant frequency is correlated with dH/dX being positive. It is interesting to note that the subharmonic dominates the flow regardless of the frequency at which the flow was forced (figure 13), the emergence of the subharmonic may thus be an inherent mechanism of the reattachment process.

It was anticipated that the imposed two-dimensional perturbations will increase the spanwise dimensions of the large coherent structures at the outer edges of the separated boundary layer. The spanwise extent of the eddies can be assessed by measuring the cross specra of the u-fluctuations at various delta Z] separation distances and calculting the coherence and the phase of the averaged data. The measurements were done at one streamwise location [i.e. at X=300mm from the apex of the wedge] for a variety of distances from the surface of the plate with and without external excitation. The comparison between the excited and unexcited flow was made at Y locations at which the mean velocity $\frac{U}{U_{init}}$ was identical regardless of the fact whether the flow was separated or not Some samples of the data are shown in figures 14a-d. Each column in these figures represents the coherence (plotted on top), the normalized amplitude of the cross-spectrum in the center and the phase is plotted below the amplitude. The frequency range of the plots is between 0-150hz. Two typical time series of the velocity signal are plotted at the bottom of each column for reference. Each column of plots represents data collected at a specific X,Y coordinate for a prescribed delta Z which is specified below.

The effect of forcing on the coherence is minimal at small separation distances even inside the

turbulent region. Outside the turbulent region $\left(\text{where } \frac{U}{U_{init}} = 1\right)$ the maximum coherence level is not affected by the forcing (see figure 15) except for the fact that the frequency corresponding to the maximum coherence in the unforced case is generally lower and it drops somewhat with increasing delta Z. The effect of forcing is strong near the solid surface. For example, at the Y location corresponding to $\frac{U}{U_{init}} = 0.3$ the maximum coherence in the forced case decays much slower with delta Z than in the unforced case. At delta Z>60mm the ratio between the forced and unforced maximum coherence is approximately double (see figure 15). For both small [delta Z<25mm] and large [delta Z>80mm] separation distances the dominant amplitudes of the cross spectrum correspond to frequencies which are lower than the forcing frequency of 42hz, however, for small delta Z the two signals are in phase while for large delta Z there is a large phase jitter between the signals. In the intermediate separation range which corresponds to approximately one half of the streamwise wavelenth of the forced oscillation the maximum coherence is dominated by the forced perturbation and the phase scrambling at all frequencies which are lower than the forced frequency is supressed. The supression of the phase jitter may be responsible for the control which is exercised by the forcing.

CONCLUSIONS

This note represents some preliminary measurements in which a successful attempt was made to control and delay the separation of a turbulent boundary layer. The introduction of harmonic, two-dimensional oscillations results in a reattachment of the flow and changes the proportions between the "wake" and the "wall" functions whose linear combination represents the streamwise velocity distribution in a turbulent boundary layer. It does not, however, alter the universal form of these functions. A detailed parametric study of the ensuing flow and the conditions for reattachment, as well as an analysis based on the stability approach, are currently under way.

REFERENCES

1. Neuburger, D. and Wygnanski, I. (1987) The use of a vibrating ribbon to delay separation on two-dimensional airfoils--preliminary observations. AFOSR Workshop on Unsteady Separated Flow, F.J. Seiler Res. Labs. report TR88-0004
2. Neuburger, D. (1988) An active delay of separation on two-dimensional airfoils. M.S thesis, Tel-Aviv University, Tel-Aviv, Israel.
3. Oster, D., Wygnanski, I., Dziomba, B., and Fiedler, H. (1978) The forced mixing layer between parallel streams in structure and mechanism of turbulence. In H. Fiedler (ed.), Lecture Notes in Physics, Vol. 75, Springer.
4. Shepshelovich, M., Koss, D., Wygnanski, I., and Seifert, A. (1989) An experimental Evaluation of a Low Reynolds Number High Lift Airfoil with Vanishingly Small Pitching Moment AIAA paper AIAA-89-0538.
5. Brown, G. L. and Roshko, A. (1974). J. Fluid Mech., Vol 64, p. 775.
6. Champagne, F. H., Pao, Y. H., and Wygnanski, I. (1976) J. Fluid Mech., Vol. 74, p. 209.
7. Gaster, M., Kit, E., and Wygnanski, I. (1985) J. Fluid Mech., Vol. 150, p. 23.
8. Sandborn, V. A. and Kline, S. J. (1961) Trans. ASME, J. of Basic Eng., Sept. 1961, p. 317.
9. Bradshaw, P. (1967) J. Fluid Mech., Vol. 29, p. 625.
10. Patrick, W. P. (1986) Flow field in a separated and reattached flat plate turbulent boundary laeyr. United Technologies Res. Center Report R85-915555.
11. Coles, D. (1956) J. Fluid Mech., Vol. 1, p. 191.

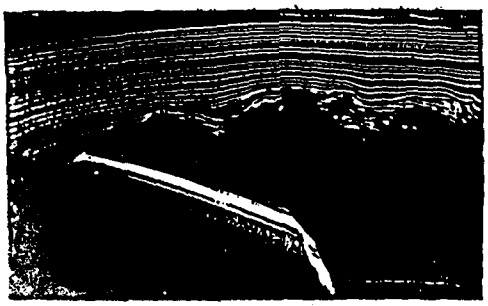

a

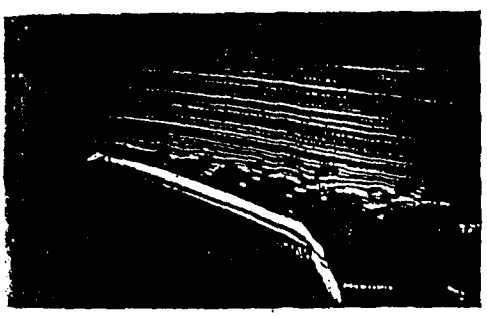

b

Fig. 1 The flow around an airfoil at an angle of incidence of 16°. Courtesy of D. Neuburger. (A small flap is visible near the leading edge).
a) The flap is stationary - flow separated.
b) The flap oscillated - flow reattached.

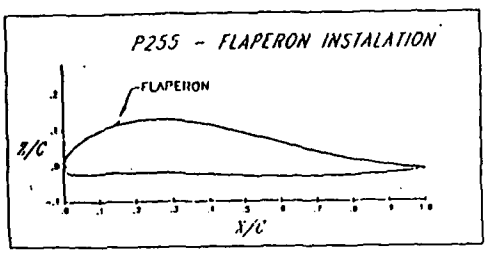

a

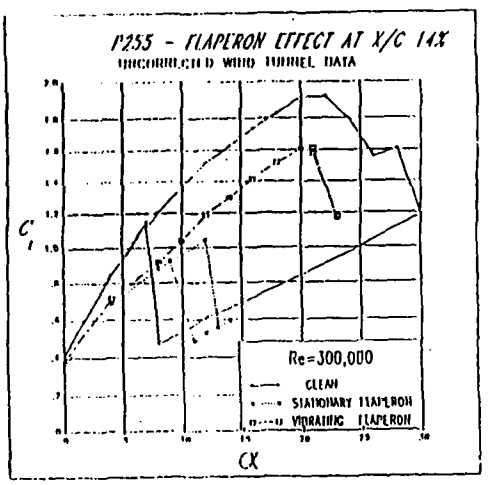

b

Fig. 2a IAI airfoil P255
2b The variation of C_L with α on the P255 airfoil and the use of a "flaperon" at Re = $3*10^6$.

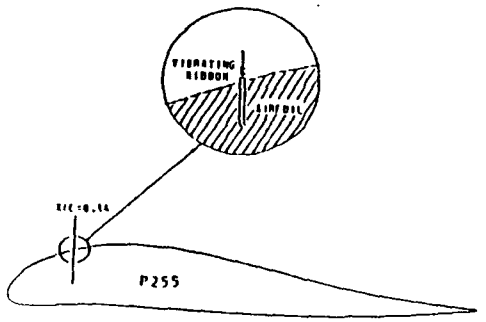

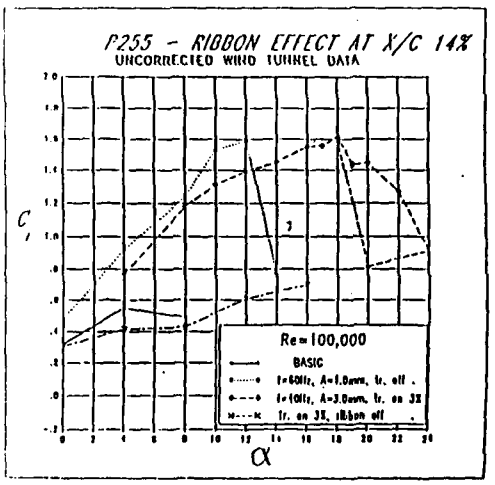

Fig. 3 The variation of C_L with α on the P255 airfoil at Re = 10^6 and the use of a vibrating fence.

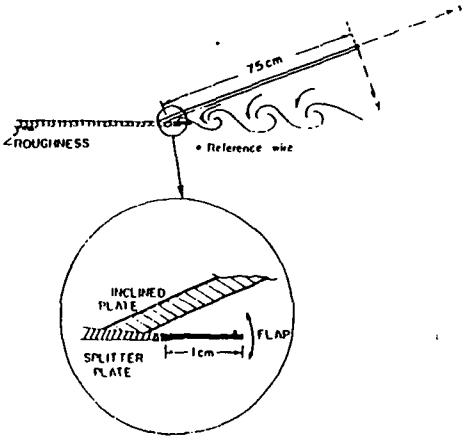

Fig. 4 A schematic diagram of the experiment.

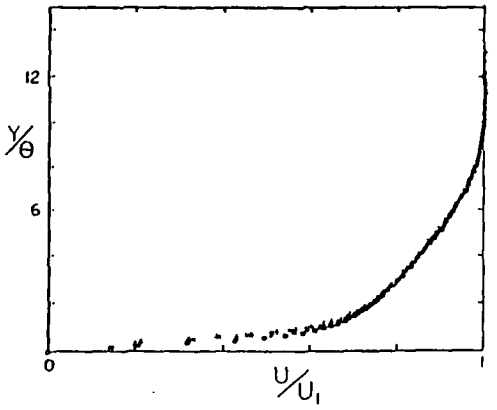

Fig. 5 The velocity profile in the upstream boundary layer - a check on the two dimensionality of the flow.

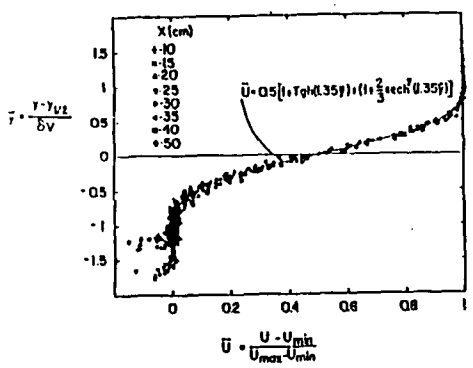

Fig. 6 The velocity distribution in the separated shear layer.

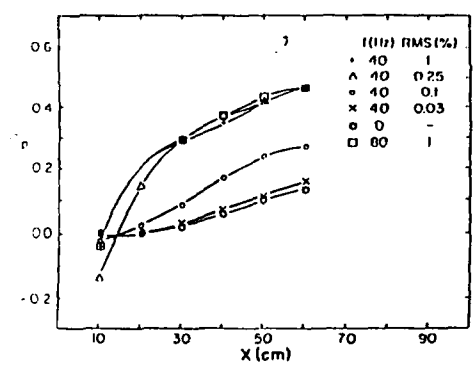

Fig. 7 The pressure distribution along the plate for various frequencies and amplitudes of excitation.

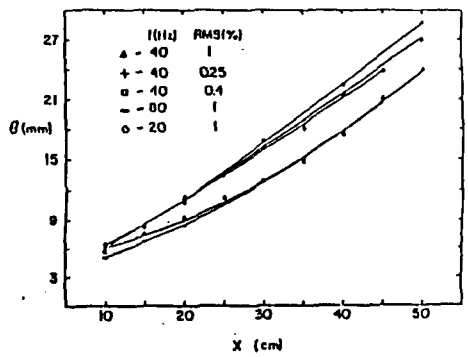

a

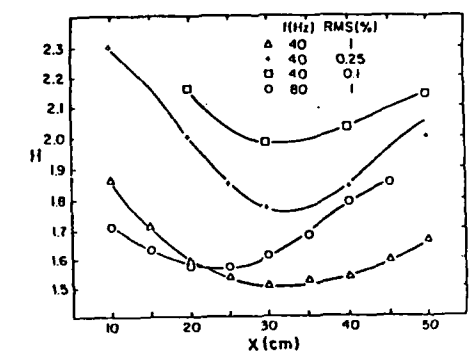

b

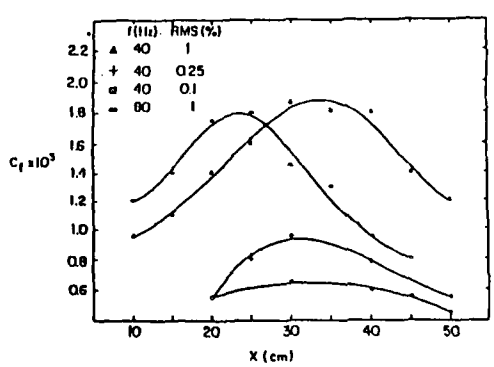

c

Fig. 8 The variation of θ, H and C_f with x for various frequency and amplitude of excitation.

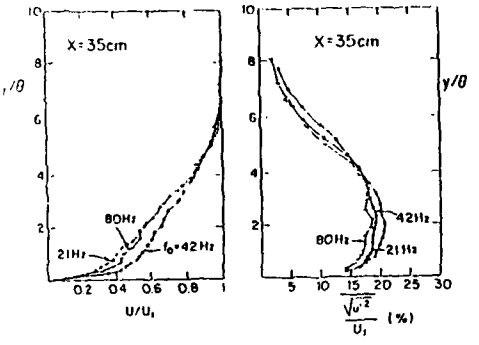

Fig. 9 Mean velocity and turbulent intensity profiles measured at x = 35 cms when the reference amplitude of the excitation was 1%.

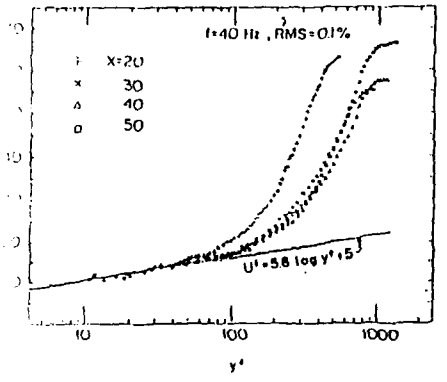

Fig. 11 The velocity profile in a partially separated flow.

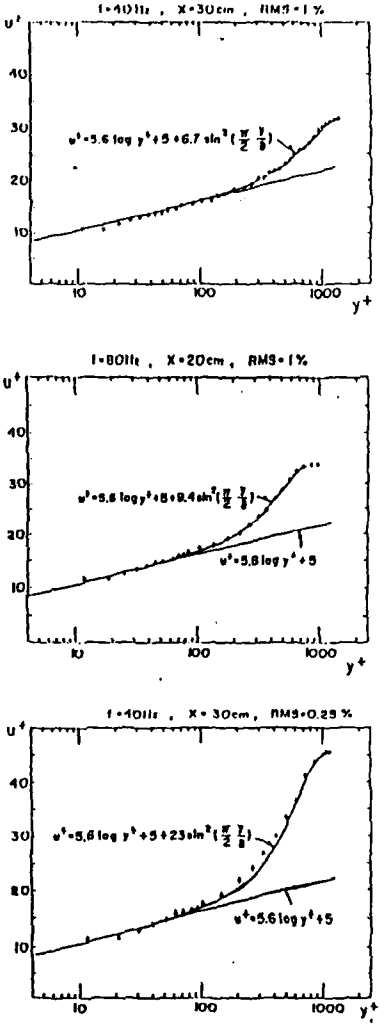

Fig. 10 Typical mean velocity profiles in the reattached boundary layer plotted in the wall coordinates.

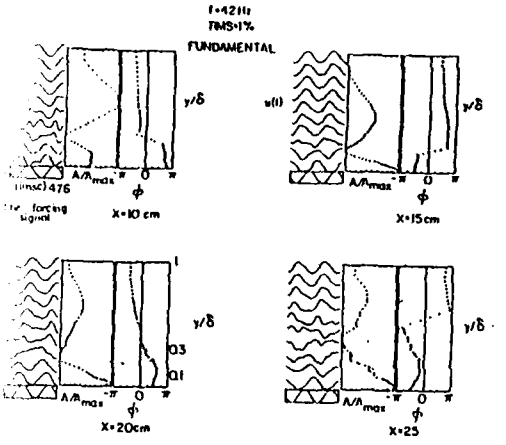

Fig. 12 The dependence of the ensemble averaged velocities on the oscillations of the flap, and the amplitude and phase distribution of the fundamental perturbation.

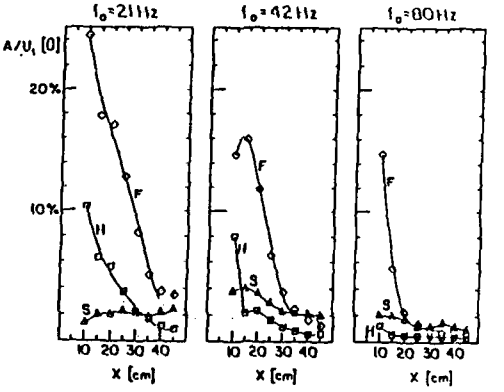

Fig. 13 The variation of the maximum amplitudes of the coherent velocity perturbations (F-fundamental frequency H-first harmonic S-subharmonic).

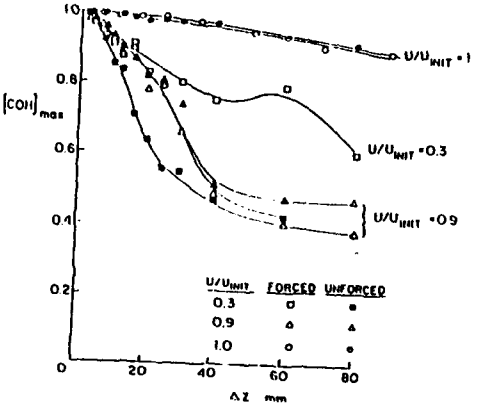

Fig. 15 A comparison between the forced and unforced $[COH]_{max}$ as a function of ΔZ.

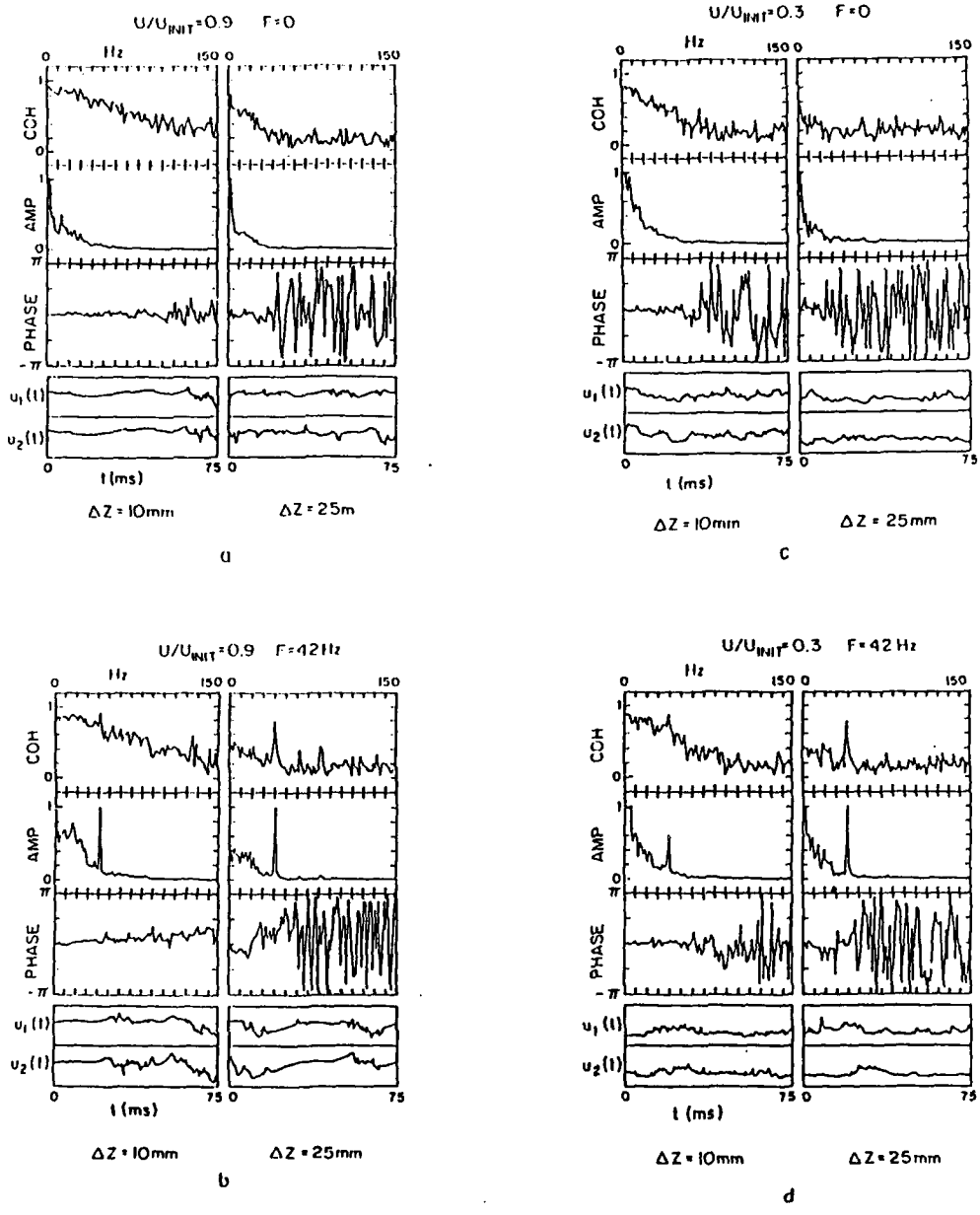

Fig. 14 Spanwise coherence amplitude of the cross spectrum and phase at various Y locations in the flow and for various separation distances ΔZ.